Homogenisation of a Folded Sandwich Core Structure

Holger Massow and Wilfried Becker

***Abstract*—** Folded cores are a not so common kind of sandwich core materials. These folded core structures have properties that make a more detailed examination advisable. Especially some properties make them particularly interesting for the aviation industry. This contribution gives an overview of the possible applications of folded core structures. By applying a numerical homogenisation method mechanical properties of folded sandwich cores are identified. For a selected type of folded core the properties are exemplarily determined. The shown homogenisation procedure is applicable to other types of sandwich cores as well. The mechanical properties presented in this contribution will be similar for other kinds of folded sandwich cores.

***Keywords*—**auxetic material, folded core, homogenisation, effective properties.

I. Introduction

IN many fields of engineering sandwich structures are quite common due to their superior characteristics in regard of effective stiffness and strength. This is in particular the case in aerospace engineering, but also in truck manufacturing, in shipbuilding and meanwhile also in civil engineering.

The typical sandwich structure is a three-layer structure, with two thin outer face sheets and a thicker core. In general the face sheets are of a relatively dense, stiff and strong material whereas the core is of low effective density, with high compliance and low strength. In aerospace industry typical cores are hard foams, honeycomb or balsa wood.

II. Folded Sandwich Cores and Possible Applications

Folded cores are a relatively novel kind of sandwich core structures. The core is manufactured by folding a planar base material into a three-dimensional structure. This process enables several geometric shapes of folded cores. Figure 1 shows two examples manufactured by the Institut für Flugzeugbau Stuttgart.

Folded cores have different advantages over other core materials. Finally, the folded cores can be manufactured by means of a continuous folding process. Compared to common honeycomb production processes a folded core can be manufactured cost-efficiently as shown in [1]. Folded cores can be made from different bulk materials e.g. aramid paper, aluminium, CFRP. Secondly, the geometry of the different folded core cells can be variable. Thereby cores with varying thickness or curved structures can be produced without post-processing [2].

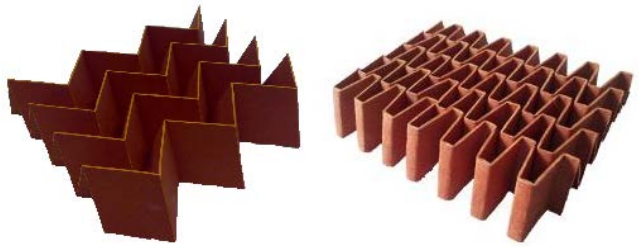

Fig. 1: Different kinds of folded sandwich cores

Another advantage, particularly for the aerospace industry, is that the folded core is open and can be ventilated (figure 2). The use of closed cell sandwich structures like honeycomb is problematic for exterior structural components. There is the problem of the diffusion-induced penetration of moisture and condensation of water. The water can be discharged only poorly. By using ventilated folded cores the problem could be solved [1].

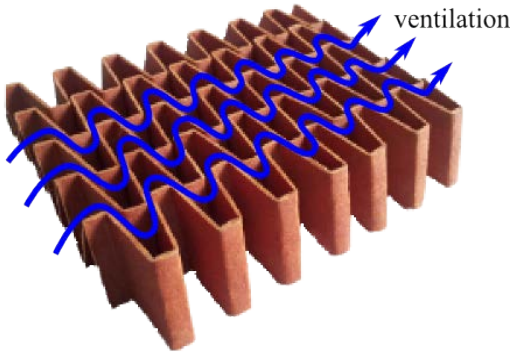

Fig. 2: Ventilation of the folded sandwich core

The possibility to ventilate the folded sandwich core also enables boundary layer suction. The channels of the folded core could be used for the suction (figure 3). In chordwise direction, the pressure in the folded core can be controlled by differently sized holes [3].

Holger Massow is with the Institute of Structural Mechanics, TU Darmstadt, Darmstadt, 64287 Germany (e-mail: massow@fsm.tu-darmstadt.de).

Wilfried Becker, is with the Institute of Structural Mechanics, TU Darmstadt, Darmstadt, 64287 Germany (corresponding author phone: +496151 1626140; fax: +496151 1626142; e-mail: becker@fsm.tu-darmstadt.de).

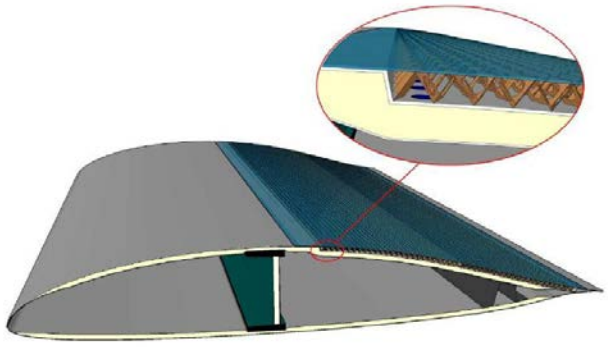

Fig. 3: Boundary layer suction by using folded sandwich core [4]

Another possible area of application is stealth technology. Folded cores have groups of faces sloped at an angle to the radiation source, where at the same time the outer skin can be positioned orthogonally to it. Furthermore, by re-reflecting the signal will lose its intensity [5]. The principle of operation is shown in figure 4.

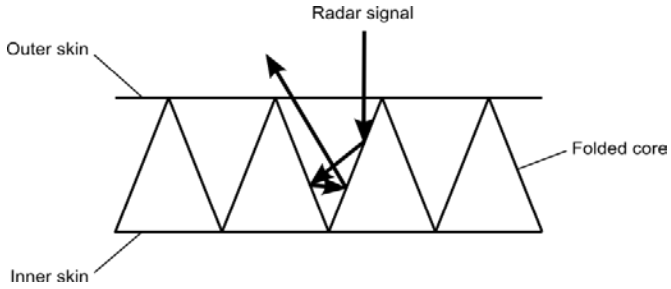

Fig. 4: Reflection of radar signal [5]

III. Homogenisation Concept

In order to use and analyse folded sandwich cores in real structural components the mechanical properties should be known. There are some publications about the mechanical properties of folded cores. Especially the behaviour under compression and shear loads [6], [7], [8] as well as the impact behaviour [9], [10] were investigated. All of these investigations however are restricted to a few geometries. There is no consideration of the general mechanical behaviour and the influence of the underlying geometric parameters. In this contribution all components of the elasticity tensor of the foldcore continuum are determined by using a numerical homogenisation concept. Furthermore, a wide range of different geometric shapes is examined.

The folded sandwich core consists of periodical wave elements. For modelling only one wave element is used as a representative volume element (RVE). It is assumed that the characteristic length L of the macro-scale structure is much larger than the characteristic length l of the considered RVE ($l<<L$) [11]. In order to determine the effective stiffness of the folded core a strain energy homogenisation concept is used [12]. In this method the assumption is made, that the RVE and a corresponding effective homogenised medium (EHM), with yet unknown properties, are equivalent, if a macroscopically equivalent deformation state leads to the same strain energy in both elements. This equivalent element is a homogeneous volume with the same shape and boundary condition as the RVE (see Fig. 5). The strain energy requires

$$\langle U \rangle = \frac{1}{V^{RVE}} \int_{RVE} U dV = \frac{1}{V^{EHM}} \int_{EHM} U^* dV = \langle U^* \rangle \quad (1)$$

where U denotes the strain energy density in the core structure and U^* the strain energy density in the equivalent homogenised medium. The equivalence of the deformation state for the elements necessitates

$$\langle F_{ij} \rangle = \frac{1}{V^{RVE}} \int_{RVE} F_{ij} dV = \frac{1}{V^{EHM}} \int_{EHM} F_{ij}^* dV = \langle F_{ij}^* \rangle \quad (2)$$

with the deformation gradient F_{ij}.

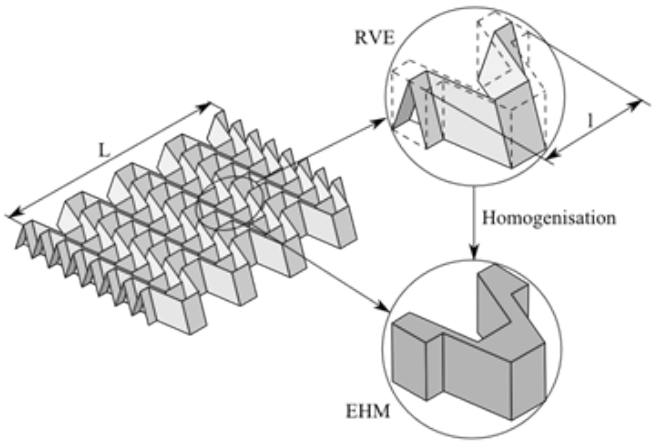

Fig. 5: Homogenisation concept for the folded core

On the outer surface of the representative volume element periodic boundary conditions are applied. This requires that the relative displacement between two points on opposite surfaces of the element is equal. This ensures that the periodic repetition of the cell is also possible in the deformed configuration. The effective Green-Lagrange strain tensor can be expressed by the deformation gradient $E_{ij} = \frac{1}{2}(F_{ki}F_{kj} - \delta_{ij})$ and it can be shown, that the effective strain tensor can be derived directly from the prescribed displacements of the corner nodes, if the translatoric and rotatory rigid body motion of the volume element is suppressed. Consequently for the determination of the effective material properties of the homogeneous medium only the displacement values at the corner nodes need to be analysed.

IV. Implementation of the Homogenisation ConCept

The numerical homogenisation is carried out with the finite element software ABAQUS. The model is generated with a PYTHON script. Also the analysis of the output data is done with the help of the PYTHON script. The folded core geometry has been generated in a parameterized form.

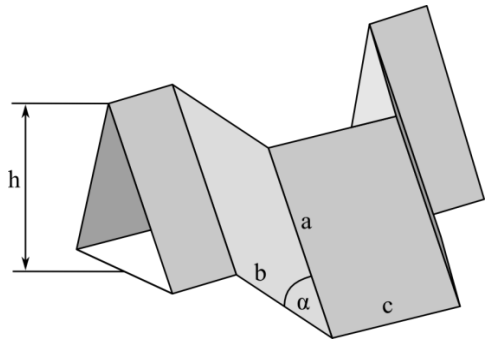

Fig. 6: Geometric parameters of the folded core

One wave element can be described by six geometric parameters (see Fig 6), namely length *a*, length *b*, length *c*, height *h*, the included angle α between edge *a* and edge *b* and the sheet thickness *t*. As starting values, the dimensions of an existing folded core (Fig.1 b, Fig. 2) are used with the following data: a = 14 mm, b = 24 mm, c = 5 mm, α = 65°, h = 19 mm and t = 0,75 mm. Due to the parameterization of the geometry, a wide selection of different configurations can be examined. For the range of parameters, there are limitations due to geometry. If the height of the folded core is zero, it becomes a flat plate. On the other hand the maximum height is calculated according to the equation:

$$h_{max} = a \cdot \sin(\alpha) \tag{3}$$

The foldcore is meshed with 4-node shell elements (S4) from the ABAQUS element library. The mesh is structured so that every node on the surface of the RVE has an opposite node that differs in only one coordinate.

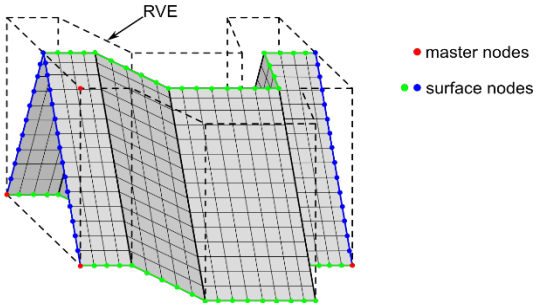

Fig. 7: The highlighted nodes of the mesh are used for the periodic boundary conditions.

By using equality constraints, periodic boundary conditions are implemented for all nodes on the outer surface of the RVE. At the corners of the volume "master nodes" are created.

All nodes on the outer surface are coupled with these "master nodes" by periodic boundary conditions of the following kind.

$$\begin{aligned} u_i^{(k+)} - u_i^{(*)} &= u_i^{(k-)} - u_i^{(1)}, \quad i = 1,2,3 \\ \varphi_i^{(k+)} &= \varphi_i^{(k-)} \end{aligned} \tag{4}$$

Therein, u_i are the translatory and φ_i the rotatory degress of freedom, *k*+ and *k*- denote corresponding nodes on opposite faces and * indicates the "master nodes" [13].

Thereby, the entire RVE can be deformed by displacements only of the master nodes. To determine all values of the elasticity tensor, it is necessary to perform three simulated "elongation tests" (see Fig. 8(a)) and three simulated "shear deformation tests" (see Fig. 8(b)) for each geometry.

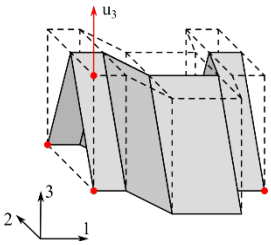

(a) Uniaxial strain deformation in 3 direction

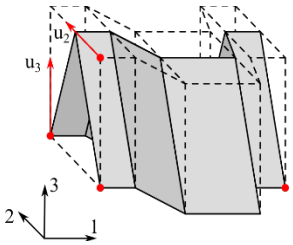

(b) Shear deformation in 23 direction

Fig. 8: Determination of the effective elasticity tensor by prescribed strain states.

V. Effective Elastic Stiffnesses

By means of the implemented homogenisation procedure all components of the elasticity tensor could be determined for a family of folded core configurations in a straightforward manner with high efficiency and generality. In doing so, the effective stiffnesses have been determined in dependence of the introduced parameters a, b, c, α, h, and t. As shown in Fig. 8 all results apply to the core without face sheets. The folded core exhibits an effective orthotropic material behaviour which can be expressed as:

$$\begin{bmatrix} \sigma_{11} \\ \sigma_{22} \\ \sigma_{33} \\ \sigma_{23} \\ \sigma_{13} \\ \sigma_{12} \end{bmatrix} = \begin{bmatrix} C_{1111} & C_{1122} & C_{1133} & 0 & 0 & 0 \\ C_{1122} & C_{2222} & C_{2233} & 0 & 0 & 0 \\ C_{1133} & C_{2233} & C_{3333} & 0 & 0 & 0 \\ 0 & 0 & 0 & C_{2323} & 0 & 0 \\ 0 & 0 & 0 & 0 & C_{1313} & 0 \\ 0 & 0 & 0 & 0 & 0 & C_{1212} \end{bmatrix} \begin{bmatrix} \varepsilon_{11} \\ \varepsilon_{22} \\ \varepsilon_{33} \\ \gamma_{23} \\ \gamma_{13} \\ \gamma_{12} \end{bmatrix} \tag{5}$$

Due to the effective orthotropic behaviour, it is possible to express the components of the stiffness tensor by the engineering constants $E_1, E_2, E_3, G_{23}, G_{13}, G_{12}, \nu_{12}, \nu_{13}, \nu_{21}, \nu_{23}, \nu_{31}$ and ν_{32}.

A. Variation of the height h

In Figs. 11-22, parametric dependences of the engineering constants are presented for three different angles α and different heights *h*. The maximum height h is obtained from Eq. (3). With the variation of the height h the orientation of the faces of the folded core varies as well. Fig. 9 shows the variation of the shape for different heights *h*.

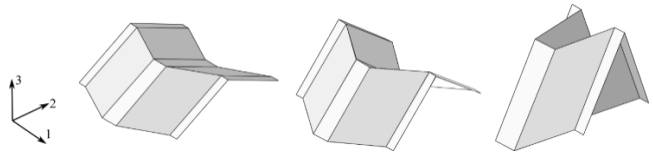

Fig. 9: Variation of the shape for different heights *h*

For each combination of the geometric parameters, respectively six simulations were executed, to determine all engineering constants. As might be expected, the effective engineering constants depend on the orientation of the faces in the RVE and the relative volume. The relative volume is defined as the ratio of the sheet volume to the RVE. There are two limiting cases for the variation of the height *h*. For the case that *h* is zero, the folded core becomes a flat sheet in the 1,2-plane. For the case that *h* is the maximum height, the faces between edge *a* and edge *b* get oriented in the 2,3-plane. These limiting cases are only theoretical cases and can only be approximated with the model.

The effects of the shape can be seen particularly well in Young's modulus E_2 (see Fig. 12). For very small heights Young's modulus converges against the material stiffness, because the faces of the folded core are almost in the 1,2-plane and the RVE corresponds to the volume of the sheet. For increasing height Young's modulus decreases, because the relative volume decreases and the orientation of the faces deviates from the 1,2-plane. If the height approaches the maximum height *h* Young's modulus again increases because the faces between edge *a* and edge *b* get orientated in the 2,3-plane.

Young's modulus E_1 (see Fig. 11) starts near the bulk material stiffness, because the faces of the folded core are almost in the 1,2-plane. Young's modulus E_1 decreases for increasing height, because the faces of the folded core move out of the 1,2-plane. The reverse behaviour can be observed for Young's modulus E_3 (see Fig. 13). Young's modulus E_3 increases for increasing height *h*, because the faces of the folded core move in the 2,3-direction.

The shear modulus G_{12} (see Fig. 14) starts near the material shear stiffness, because the faces of the folded core are almost in the 1,2-plane. The shear modulus G_{12} decreases for increasing height *h*, because the faces of the folded core move out of the 1,2 plane. The reverse behaviour can be observed for the shear modulus G_{23} (Fig. 15). The shear modulus increases for increasing height *h*, because the faces between *a* and *c* of the folded core move in the 2,3-plane.

A distinctive feature of the folded core is that the effective Poisson's ratios for some combinations of parameters can be very large compared to isotropic materials. For small heights the Poisson's ratios ν_{13} and ν_{12} become exceptionally large. Large values can be observed for large heights for the Poisson's ratios ν_{31} and ν_{32}, too. The reason for such unusual values is that the effective Poisson's ratios are dominated by the geometry. The folded core has a behaviour like a gearing mechanism. It is important to remember that only the behaviour of the core was examined without facesheets which would hinder such core behaviour.

Furthermore the effective Poisson's ratios ν_{12} and ν_{21} can be negative. Figs. 21-22 show the variation of ν_{12} and ν_{21} for different angles α. For a height *h* near zero Poisson's ratios are positive, in the extreme case $h = 0$ it would be the material Poisson's ratio. For increasing height *h* the Poisson's ratio ν_{12} becomes negative. Heuristically, this can be explained by a gearing mechanism of the foldcore structure as it is illustrated by the series of fold-configurations in the respective figures. A material with this kind of behaviour is called auxetic. This kind of behaviour means that under uniaxial tensile behaviour in the 1-direction there will be an elongation also in the 2-direction.

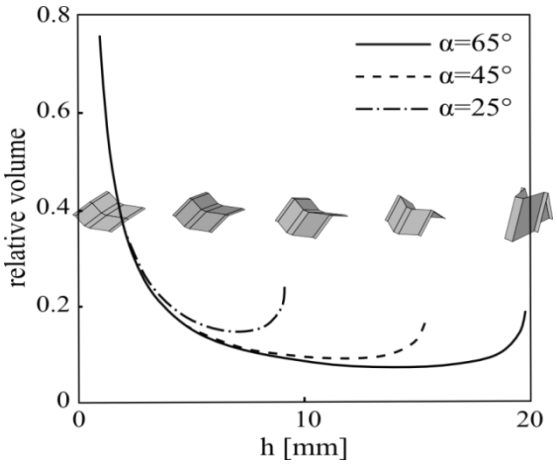

Fig. 10: Relative volume as function of core height

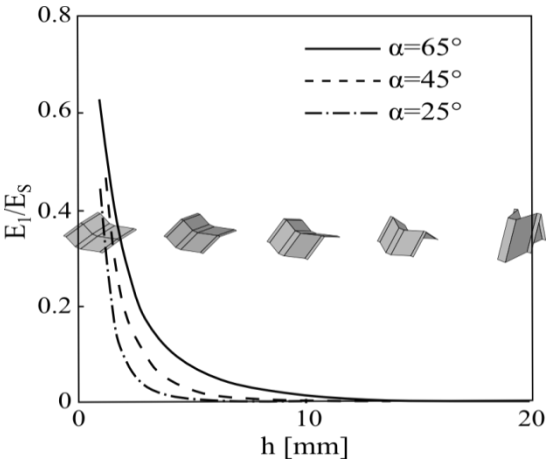

Fig. 11: Young's modulus E_1 as function of core height

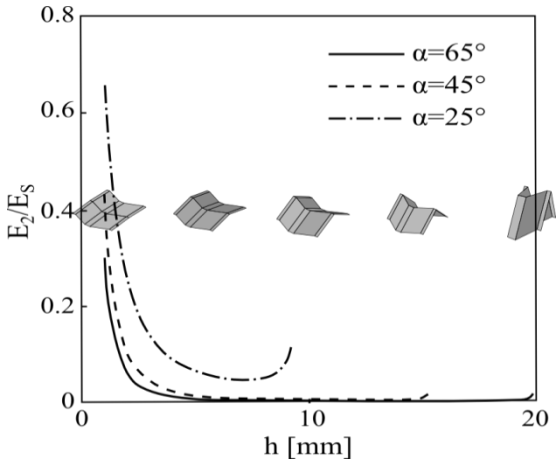

Fig. 12: Young's modulus E_2 as function of core height

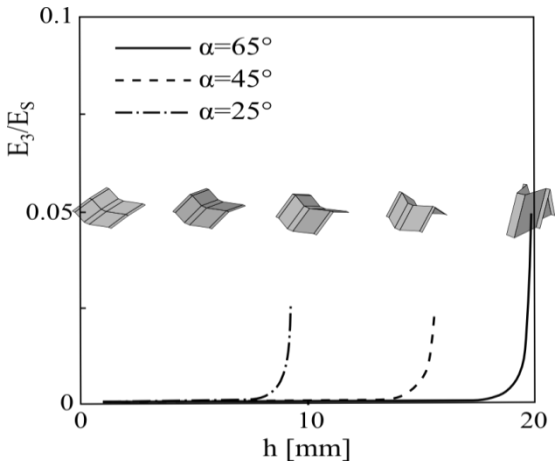

Fig. 13: Young's modulus E_3 as function of core height

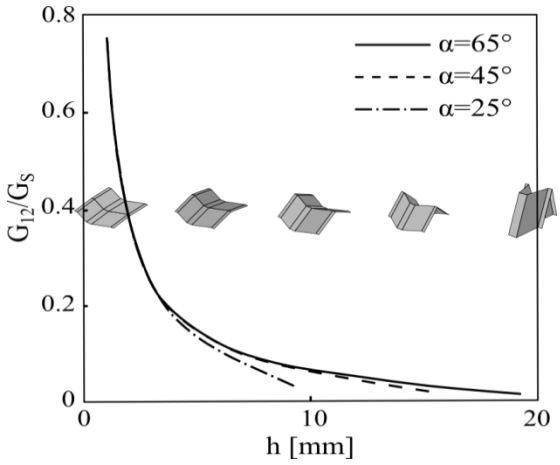

Fig. 14: Shear modulus G_{12} as function of core height

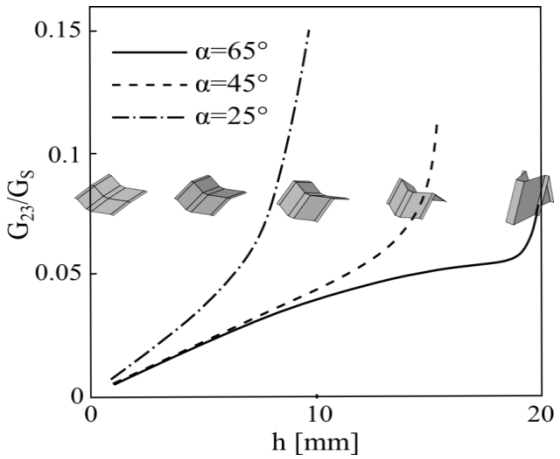

Fig. 15: Shear modulus G_{23} as function of core height

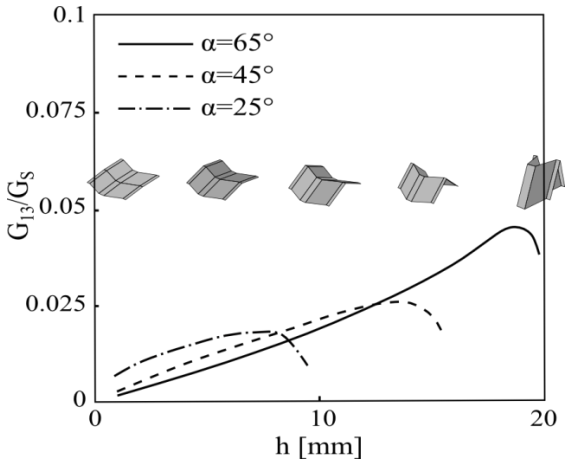

Fig. 16: Shear modulus G_{13} as function of core height

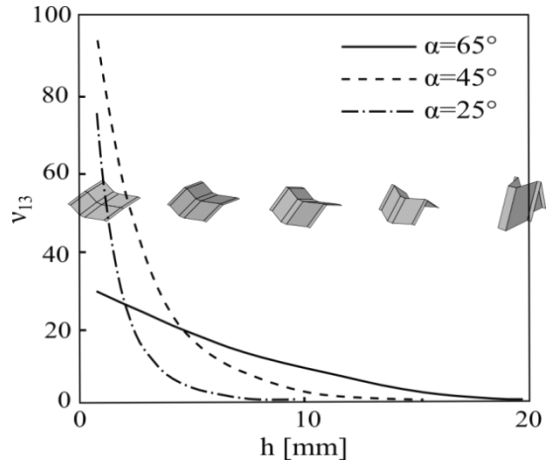

Fig. 17: Poisson's ratio ν_{13} as function of core height

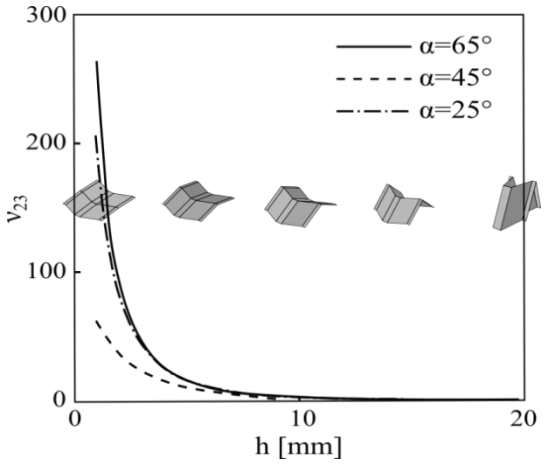

Fig. 18: Poisson's ratio ν_{23} as function of core height

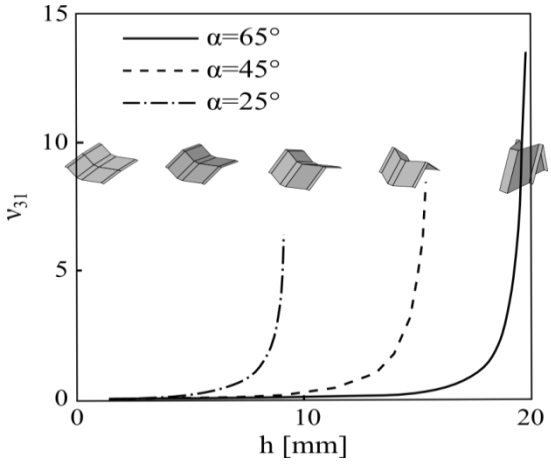

Fig. 19: Poisson's ratio ν_{31} as function of core height

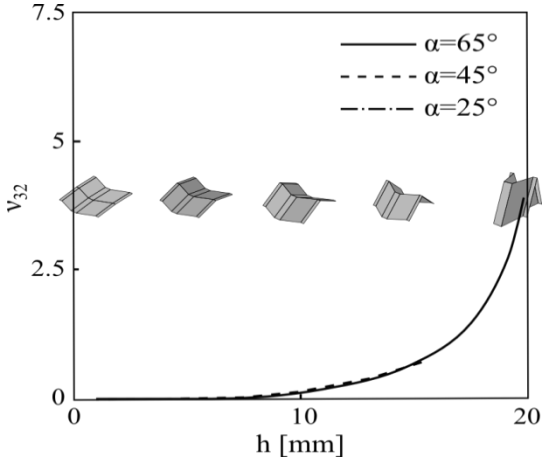

Fig. 20: Poisson's ratio ν_{32} as function of core height

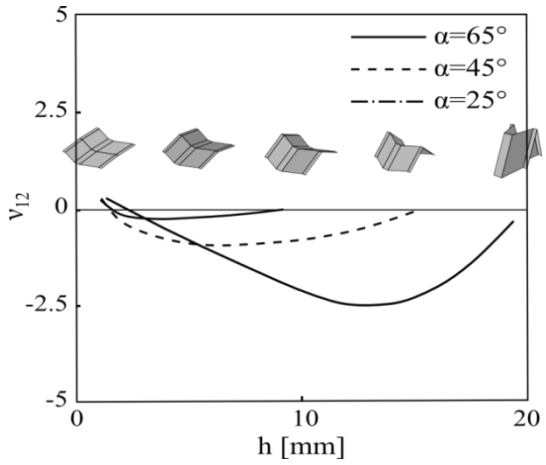

Fig. 21: Poisson's ratio ν_{12} as function core height

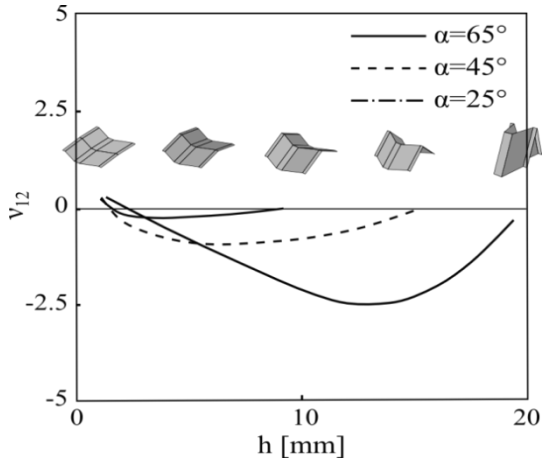

Fig. 22: Poisson's ratio ν_{21} as function of core height

B. *Variation of the angle α*

In Figs. 24-36, parametric dependences of the engineering constants are presented for four different heights *h* and different angles α. The maximum angle α is 90° and the minimum angle α is obtained by:

$$\arccos\left(\sqrt{1-\frac{h^2}{a^2}}\right) \leq \alpha \tag{4}$$

With the variation of the angle α the orientation of the faces of the folded core varies as well. Fig. 23 shows the variation of the shape for different angles α. The variation of the angle results in a significant change in the shape of the folded core. For the limiting angle α = 90°, the core becomes a prismatic wave.

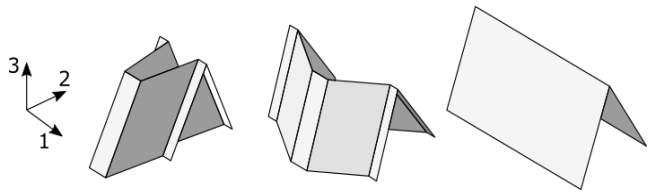

Fig. 23: Variation of the shape for different angles

Again, for each combination of the parameters, all engineering constants are determined. Also in the variation of the angle, the constants depend on the orientation of the faces in the RVE. The change of the relative volume has not such an important influence in the study before.

Young's modulus E_1 (see Fig. 24) starts at a low relative stiffness and increases with increasing angle α. This behaviour can be explained by the variation of the shape shown in Figure 23. At a small angle, the surfaces are mainly oriented in the 2 direction. With increasing angle α, the faces of the folded core change the orientation to the 1-direction. In the limiting case α = 90° all faces are orientated in the 1-direction.

Young's modulus E_2 (see Fig. 25) shows the opposite behaviour as Young's modulus E_1. The explanation is the same argumentation as before. Because of the variation of the angle α the faces change their orientations. In the limiting case α = 90° all faces are orientated in the 1-direction and Young's modulus E_2 reaches the lowest value.

Young's modulus E_3 (see Fig. 26) shows a decreasing behaviour for an increasing angle α. The reason for this behaviour is the orientation of the rhomboid shaped faces of the folded core. For the case of a small angle α these faces are almost in 3-direction. For an increasing angle α the faces move out of the 3-direction.

The shear modulus G_{12} (see Fig. 27) and shear modulus G_{13} (see Fig. 28) increase with increasing angle α. For smaller angles α the slope of the graph is very steep. The reason is that in this range a small change of the angle α causes a bigger variation of the shape of the folded core. The shear modulus G_{23} (see Fig. 29) decreases for increasing angle α. This can be explained, because the faces of the folded core move out of the 2,3-plane.

Again, Poisson's ratios of the folded core are large compared to isotropic materials. But there are not such extreme values for the Poisson's ratios ν_{13} and ν_{23}. The reason for this less extreme behaviour in the case of variation of the angle α in comparison of the variation of the height h is, that the variation of the core shape is not that much.

The reason for such unusual values is that the effective Poisson's ratios are dominated by the geometry. The folded core has a behaviour like a gearing mechanism. It is important to remember that only the behaviour of the core was examined without facesheets which would hinder such core behaviour.

Furthermore the effective Poisson's ratios ν_{12} and ν_{21} can be negative. Figs. 30 and 32 show the variation of ν_{12} and ν_{21} for the variation of the angles α. For a range of the angle α Poisson's ratios are negative. Heuristically, this can be explained by a gearing mechanism of the foldcore structure as it is illustrated figure 23.

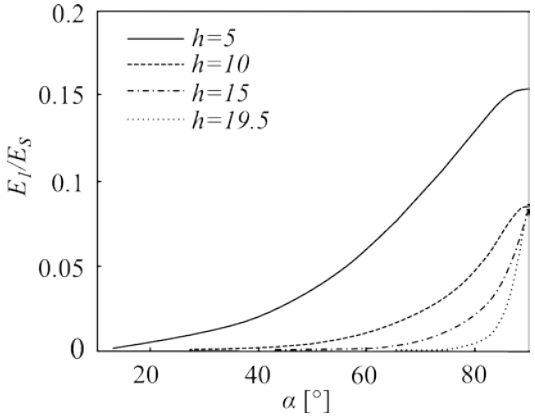

Fig. 24: Young's modulus E_1 as function of the angle α

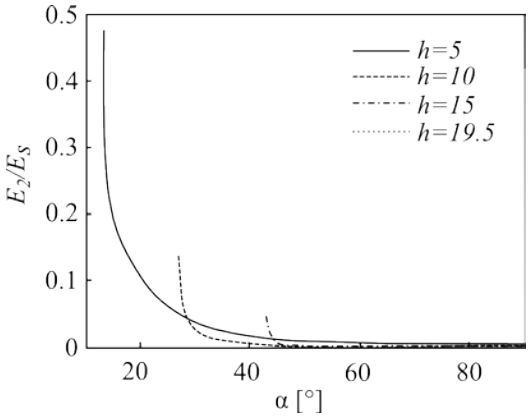

Fig. 25: Young's modulus E_1 as function of the angle α

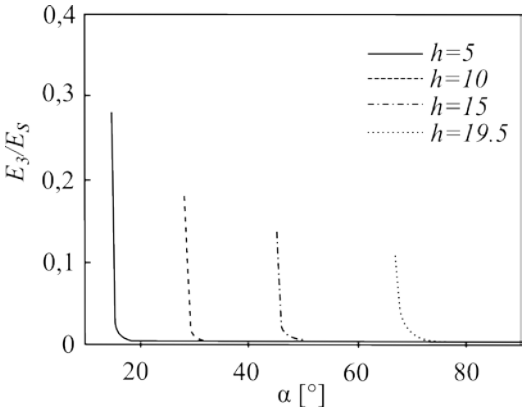

Fig. 26: Young's modulus E_3 as function of the angle α

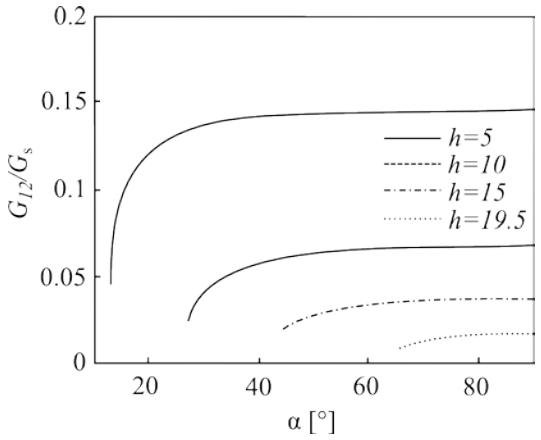

Fig. 27: Shear modulus G_{12} as function of angle α

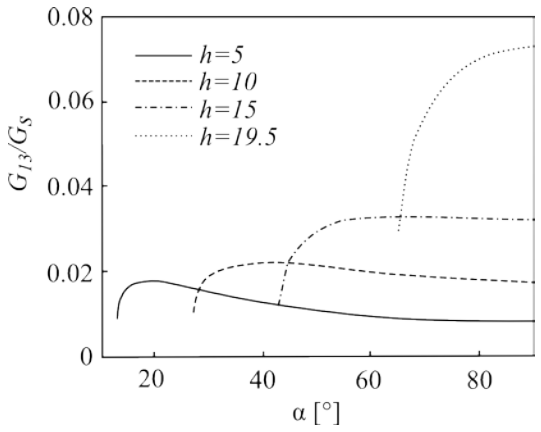

Fig. 28: Shear modulus G_{13} as function of angle α

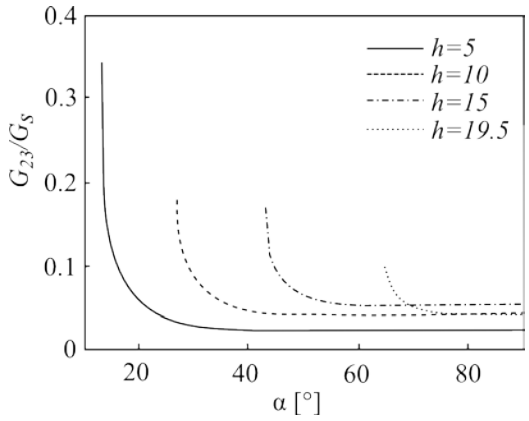

Fig. 29: Shear modulus G_{23} as function of the angle α

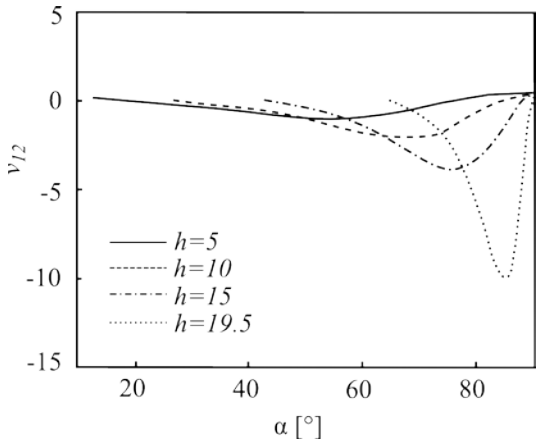

Fig. 30: Poisson's ratio v_{12} as function of the angle α

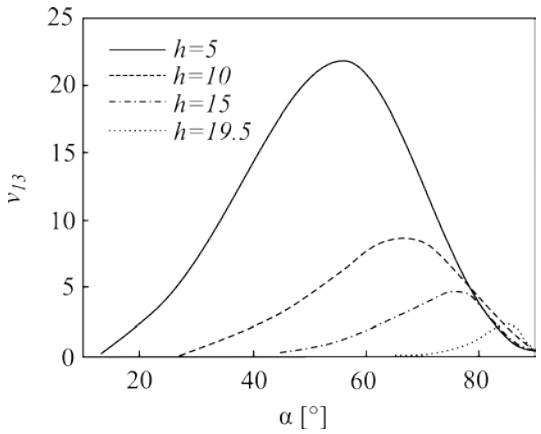

Fig. 31: Poisson's ratio v_{13} as function of the angle α

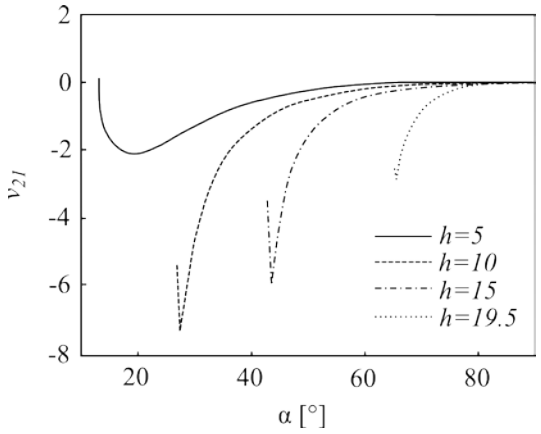

Fig. 32: Poisson's ratio v_{21} as function of the angle α

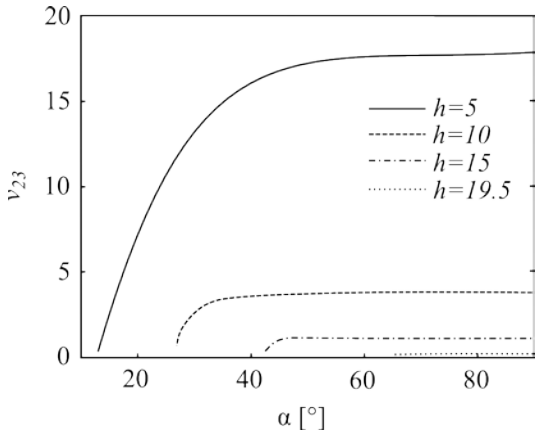

Fig. 33: Poisson's ratio ν_{23} as function of the angle α

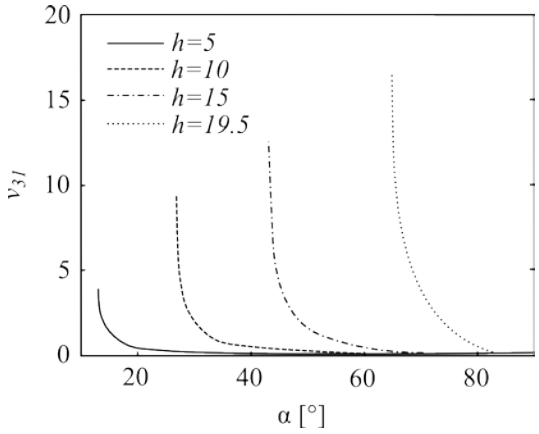

Fig. 34: Poisson's ratio ν_{31} as function of the angle α

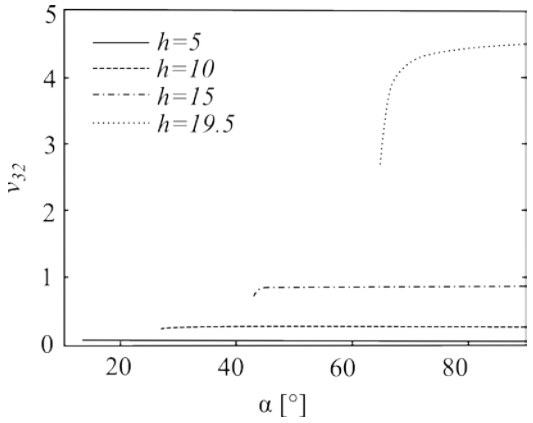

Fig. 35: Poisson's ratio ν_{32} as function of the angle α

VI. Conclusion

In many fields of modern lightweight constructions sandwich structures play an increasingly important role. By using folded core structures instead of common sandwich structures it is possible to avoid disadvantages like accumulated water in closed cells. Special applications like boundary layer suction or stealth technology are conceivable.

By the concept of a representative volume element and by the techniques of homogenisation the effective elastic properties of a sandwich core can be identified. The effective mechanical properties of an example of one type of folded core were determined for the variation of the height *h* and for the variation of the angle α. These two parameters were varied within a wide range. A technically useful range is much smaller, but for extreme cases of the geometry the folded core has astonishing properties. The foldcore exhibits two amazing effective mechanical properties, namely very large Poisson's ratios and negative Poisson's ratios.

References

[1] K. Drechsler and R. Kehrle, Manufacturing of folded core structures for technical applications, *SAMPE Europe 25th International Conference*, Paris, France, 2004, pp. 508-513.

[2] S. Fischer, S. Heimbs, S. Kilcher, M. Klaus and C. Cluzel, Sandwich structures with foldcore: manufacturing and mechanical behavior, *SAMPE Europe International Conference*, Paris, France, 2009.

[3] M. Gogl, *Aerodynamic Design of a Sailplane Wing with Boundary Layer Suction*, Idaflieg Berichtsheft, 23, 2013.

[4] L. M. M. Boermans, *Research on sailplane aerodynamics at Delft University of Technology. Recent and present developments.* NVvL, Delft, Netherland, 2006.

[5] V. I. Khaliulin, A. V. Shabalov, Applicability of Folded Structures for Enhancement of Helicopter Radar Transparency, *33rd European Rotorcraft Forum*, Kazan, Russia, 2007.

[6] L. P. Shabalin, A. V. Gorelov, I. N. Sidorov, V. I. Khaliulin and I. V. Dvoyeglazov, Calculation of the parameters of stress-strain and ultimate states of composite foldcores under transverse compression and shear, *Mechanics of Composite Materials*, Vol. 48, No. 4, 2012.

[7] S. Kilchert, *Nonlinear finite element modeling of degradation and failure in folded core composite sandwich structures*, dissertation, Universität Stuttgart, Stuttgart, 2013.

[8] S. Fischer, *Numerische Simulation der mechanischen Eigenschaften von Faltkern-Sandwichstrukturen*, dissertation, Universität Stuttgart, Stuttgart, 2012.

[9] S. Heimbs, J. Cichosz, S. Kilchert and M. Klaus, Sandwich panels with cellular cores made of folded composite material: mechanical behaviour and impact performance, *17th International Conference on Composite Materials*, Edinburgh, UK, 2009.

[10] S. Heimbs, P. Middendorf, C. Hampf, F. Hähnel and K. Wolf, Aircraft Sandwich Structures with folded Core under Impact Load, *Composite Solutions, AeroSpace*, Vol. 3, No. 3, 2009, pp. 7-13.

[11] D. Gross and T. Seelig, *Fracture Mechanics. With an Introduction to Micromechanics*, Springer, Berlin, Germany, 2011.

[12] J. Hohe and W. Becker, Effective mechanical behavior of hyperelastic honeycombs and two-dimensional model foams at finite strain, *International Journal of Mechanical Sciences*, 45, 2003, pp.. 891-913.